

# RNA splicing promotes translation and RNA surveillance

Jayanthi P Gudikote, J Saadi Imam, Ramon F Garcia & Miles F Wilkinson

**Aberrant mRNAs harboring premature termination codons (PTCs or nonsense codons) are degraded by the nonsense-mediated mRNA decay (NMD) pathway. mRNAs transcribed from genes that naturally acquire PTCs during lymphocyte development are strongly downregulated by PTCs. Here we show that a signal essential for this robust mRNA downregulatory response is efficient RNA splicing. Strong mRNA downregulation can be conferred on a poor NMD substrate by either strengthening its splicing signals or removing its weak introns. Efficient splicing also strongly promotes translation, providing a molecular explanation for enhanced NMD and suggesting that efficient splicing may have evolved to enhance both protein production and RNA surveillance. Our results suggest simple approaches for increasing protein expression from expression vectors and treating human genetic diseases caused by nonsense and frameshift mutations.**

NMD degrades aberrant mRNA transcripts harboring PTCs<sup>1–4</sup>. PTCs are common in mRNAs, as they arise not only from mutant genes that contain nonsense and frameshift mutations, but also from wild-type genes, where they result from splicing and transcription errors. Eliminating such aberrant mRNAs is important, as they can encode proteins with dominant-negative or deleterious gain-of-function effects<sup>1,4,5</sup>.

Although the underlying mechanism for NMD is just beginning to be elucidated, one feature that is already clear is that it requires RNA splicing. Work performed by several laboratories has shown that mammalian NMD requires not only a stop codon but also a downstream intron. The requirement for a downstream intron as a second signal to elicit NMD is supported by several lines of evidence: (i) removal of the introns downstream from PTCs abrogates NMD<sup>6</sup>; (ii) addition of introns downstream from a normal stop codon elicits NMD<sup>3,6</sup>; and (iii) naturally intronless mammalian mRNAs are not substrates for NMD<sup>7,8</sup>.

A downstream intron is a logical NMD second signal, as normal stop codons are usually located in the final exon and hence do not trigger NMD. However, the question of how introns could participate in NMD at the mechanistic level was initially puzzling, as introns are already spliced out when fully spliced mRNAs are scanned for stop codons by the cytoplasmic translational machinery. Recently, this problem was solved when it was discovered that after splicing the spliceosome leaves behind a 'mark' that serves as the proximal second signal for NMD<sup>3,9,10</sup>. This mark, called the exon-junction complex (EJC), is a set of proteins deposited ~20–24 nucleotides (nt) upstream of each exon-exon junction.

T-cell receptor- $\beta$  (TCR $\beta$ ) and immunoglobulin mRNAs are transcribed from genes that acquire PTCs two-thirds of the time as a result of programmed DNA rearrangements during normal lymphocyte development. The frequent acquisition of PTCs may have led to strong selection pressure to effectively rid lymphocytes of PTC-bearing

TCR $\beta$  transcripts<sup>1,4,11</sup>. Consistent with this, TCR $\beta$  transcripts harboring PTCs are downregulated much more (to ~1–5% of normal levels) than are transcripts from nonrearranging genes (to ~10–30% of normal levels)<sup>11,12</sup>. Previously, we have shown that this strong downregulatory response is neither cell-type nor promoter specific<sup>12</sup>. Instead, we found that a region in the TCR $\beta$  gene encompassing the rearranging VDJ exon and the adjacent intronic sequences conferred this property. Here, we set out to identify the specific sequences responsible. We report that strong downregulation of PTC-bearing mRNAs is elicited by sequences that promote efficient RNA splicing.

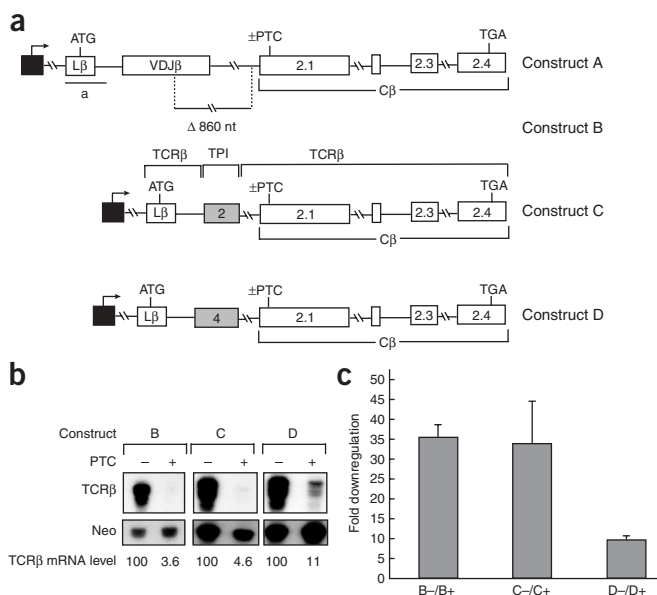
## RESULTS

### Strong mRNA downregulation without the VDJ exon

Previously, we showed that deleting the VDJ exon and the adjacent intronic sequences reduced the magnitude of TCR $\beta$  NMD<sup>12</sup>. To investigate whether a specific *cis* element in the TCR $\beta$  VDJ exon is responsible for this, we deleted several regions of the VDJ exon. We found that these deletions did not have a substantial effect on NMD (compare A-/A+ with B-/B+, P-/P+ and Q-/Q+ in **Supplementary Fig. 1** online). Although this ruled out the existence of a single VDJ exon element essential for strong mRNA downregulation, it remained possible that redundant *cis* elements existed in this exon, any one of which could elicit strong mRNA downregulation. To test this possibility, we replaced the VDJ exon with an exon from another gene. We chose to use an exon from the TPI gene because transcripts from this well-studied gene undergo only modest (three- to four-fold) NMD<sup>12,13</sup>. In particular, we chose TPI exon 2 (**Fig. 1a**, construct C), as its length (124 nt) is similar to that of the 5' half of the VDJ exon (162 nt), which we showed to be sufficient to drive robust NMD (construct B in **Fig. 1a** and **Supplementary Fig. 1**). PTC-bearing (PTC+) and PTC-lacking (PTC-) versions of this TPI-TCR $\beta$  chimeric gene were transiently transfected into HeLa cells. HeLa cells were used

Department of Immunology, University of Texas M.D. Anderson Cancer Center, Houston, Texas 77030, USA. Correspondence should be addressed to M.F.W. (mwilkins@mdanderson.org).

Published online 21 August 2005; doi:10.1038/nsmb980



because they transfect efficiently and they reproduce all known aspects of TCR $\beta$  NMD that occur in T cells<sup>6,14</sup>. Northern-blot analysis showed that the TPI-TCR $\beta$  chimeric construct expressed a transcript of the expected size ( $\sim 1.1$  kilobases (kb); data not shown). RNase protection analysis (RPA) showed that the presence of a PTC decreased the levels of transcripts from this TPI-TCR $\beta$  chimeric gene and of transcripts from the parental gene by the same magnitude (Fig. 1b, B-/B+ versus C-/C+). Transcripts from both were downregulated more than 30-fold (Fig. 1c). We conclude that the TCR $\beta$  VDJ exon is not essential for strong mRNA downregulation in response to PTCs.

To determine whether any exon at this position was compatible with strong downregulation, we substituted another TPI exon (TPI exon 4) that is 134 nt long, a length similar to that of TPI exon 2. We found that transcripts from this chimeric gene (construct D, Fig. 1a) were only moderately downregulated (about nine-fold) when they contained a PTC (Fig. 1b,c). Although the degree of downregulation was much higher than that seen with transcripts from the full-length TPI gene (about three-fold), it was not as high as that seen with the parental TCR $\beta$  transcripts ( $\sim 35$ -fold) or TPI exon 2-TCR $\beta$  chimeric transcripts ( $\sim 33$ -fold; Fig. 1b,c). This shows that although the VDJ exon is not essential for strong mRNA downregulation, the particular exon sequences chosen to replace the VDJ exon can affect the magnitude of mRNA downregulation.

### Inefficient splicing weakens mRNA downregulation

To assess why TPI exons 2 and 4 might differ in their ability to elicit robust downregulation, we compared their sequences. Using a program that identifies exonic splicing enhancer (ESE) consensus sequences<sup>15</sup>, we discovered that TPI exon 2 has a much higher density of putative ESEs (17 ESEs per 100 nt) than does TPI exon 4 (11 ESEs per 100 nt). This suggested the hypothesis that efficient splicing elicits strong downregulation of mRNAs that contain PTCs. Consistent with this hypothesis, the ESE density in TPI exon 2 is the same as that in the TCR $\beta$  VDJ exon, which also triggers robust mRNA downregulation. In addition, we found that the introns in the V $\beta_{8.1}$  D $\beta_2$  J $\beta_{2.3}$  TCR $\beta$  gene have consensus or nearly consensus splice sites (Table 1).

We directly tested this hypothesis by making splice-site mutations predicted to reduce splicing efficiency. We did not attempt to alter

**Figure 1** The VDJ exon is dispensable for strong downregulation of mRNAs that contain a PTC. (a) Schematic diagram of the wild-type (A) and chimeric TCR $\beta$  constructs driven by the  $\beta$ -actin promoter (black box). In the chimeric constructs, the TCR $\beta$  VDJ exon was substituted with either TPI exon 2 (C) or TPI exon 4 (D), with or without a PTC in the C $\beta$ 2.1 exon ( $\pm$ PTC). Construct B harbors the deletion shown. Probe a (denoted by lower-case 'a' below the diagram) protects 139 nt of pre-mRNA and 73 nt of spliced mRNA. ATG, start codon; TGA, stop codon. (b) Results of RPA (using probe a) of total RNA (10  $\mu$ g) isolated from HeLa cells transiently transfected as previously described<sup>12</sup> with 2  $\mu$ g of the constructs shown. TCR $\beta$  mRNA levels given are relative to PTC- mRNA levels (PTC- levels for each type of construct are set to 100). TCR $\beta$  mRNA levels were normalized for differences in transfection efficiency and RNA loading by measuring the level of neomycin (Neo) mRNA, which is expressed as a separate transcription unit from the plasmids in panel a. (c) Ratio of PTC- to PTC+ mRNA levels (fold downregulation). Values are means of three independent transfection experiments. Error bars, s.d.

RNA splicing rates by mutating ESEs, as they tend to be redundant and are therefore difficult to inactivate. We decided first to make splice-site mutations in intron 2 (IVS2), as the exon downstream of it (C $\beta$ 2.1) had strong consensus splice sites on either side of it (Table 1). We made pyrimidine-to-purine substitutions at the -6 and -3 positions in its 3' splice site (Fig. 2a, construct F), which resulted in a much lower calculated splice-site score (82.3) than for the wild-type intron (96.0). To assess whether this double mutation inhibited splicing, we determined the ratio of mature mRNA to pre-mRNA, a measure of the *in vivo* splicing rate<sup>16</sup>. This analysis showed that IVS2 splicing was inhibited, as were splicing of the upstream and downstream introns (Fig. 2b-d). As further evidence of inefficient IVS2 splicing, northern-blot analysis revealed that the exon 3' of IVS2 was skipped in 50% of the mutant transcripts (data not shown).

Having shown that the double mutation effectively reduced splicing, we then determined its effect on NMD. Using a probe specific for the normally spliced transcript (Fig. 2a, probe d), we found that the splice-site mutations reduced PTC-induced downregulation of this transcript (Fig. 2e-h). Compared to wild-type transcripts, mutants showed five times less mRNA downregulation when they contained a C $\beta$ 2.1-exon PTC (Fig. 2g,h, A-/AC+ versus F-/FC+) and two to three times less mRNA downregulation when they contained a VDJ-exon PTC (Fig. 2e,f, A-/AV+ versus F-/FV+). Similar results were obtained

**Table 1** Splice-site scores for TCR $\beta$  and TPI

Gene	Intron	Donor site		Acceptor site	Acceptor site score
		Donor site	score		
TCR $\beta$	IVS1	AA GTGAGT	84.3	TTTCTTTATTACAG A	95.2
	IVS2	CG GTAAGT	91.8	TCTTTACTTTCCAG A	96.0
	IVS3	AG GTAAGT	100.0	CTCCTTTCTTTCCAG A	92.1
	IVS4	AG GTGAGT	96.7	TTTCTGTCAACAG C	87.8
	IVS5	TG GTAAGA	86.5	CTTCTCTTTCTCAG G	95.8
TPI	IVS1	CG GTAAGC	86.0	CATCTTGTCCCTCAG A	89.1
	IVS2	AG GTGAGA	91.1	ATCTCTTCTTTTAG C	80.6 <sup>a</sup>
	IVS3	AG GTTAGT	90.0	CTGTTTCTCAACAG C	88.8
	IVS4	AG GTATCT	74.5 <sup>a</sup>	TCTGTGCCCTCAG A	92.0
	IVS5	AG GTAACC	79.9 <sup>a</sup>	GCTTCTTGTCTTAG G	87.5
	IVS6	AG GTGAGT	96.7	TGCTCCCTTCCAG G	94.1
Consensus		AG GT AGT G		TT TTTT TT NCAG G CC CCCCC	

<sup>a</sup>Weaker than the weakest TCR $\beta$  splice site.

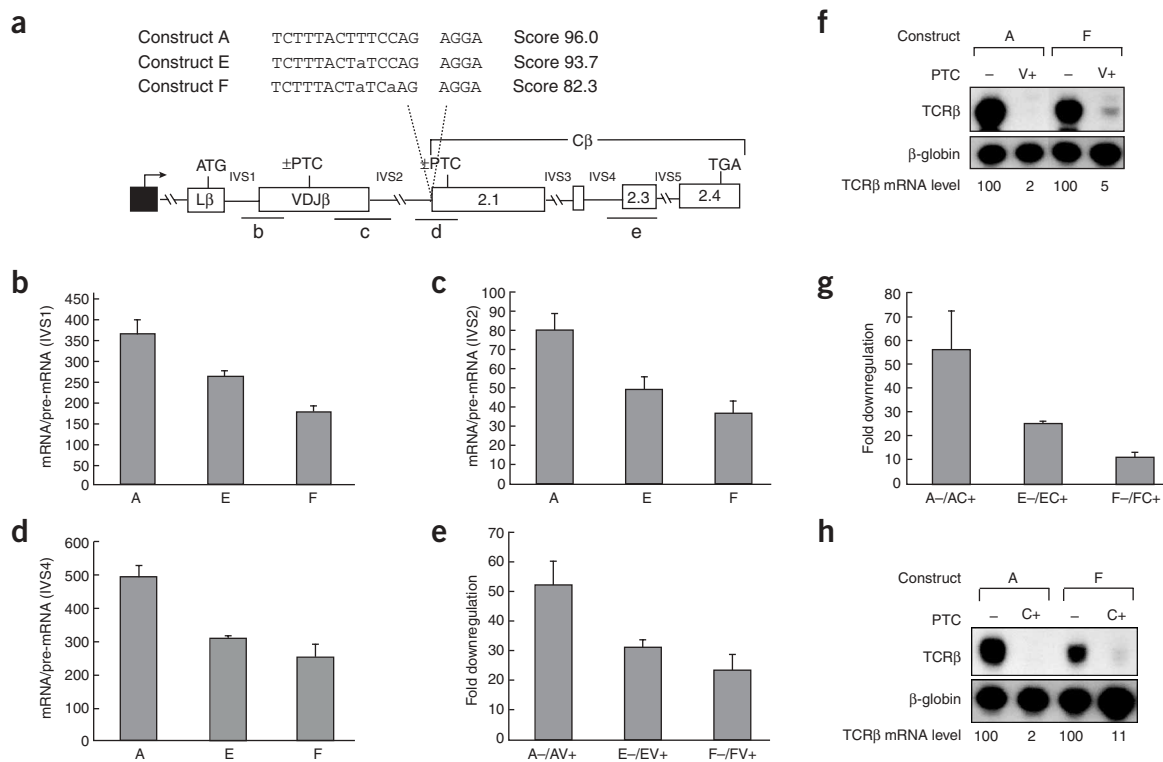


**Figure 2** Mutations in the IVS2 3' splice site reduce the downregulation of TCR $\beta$  transcripts that contain a PTC. **(a)** Schematic diagram of wild-type (A) and mutated (E and F) TCR $\beta$  constructs, with their splice-site scores and intron-exon junction sequences, including mutations (lower case). ATG, start codon; TGA, stop codon. Probes are denoted by lower-case letters below the diagram: probe b protects 134 nt of pre-mRNA and 72 nt of spliced mRNA; c protects 179 nt of pre-mRNA and 90 nt of spliced mRNA; d protects 60 nt of spliced mRNA; and e protects 152 nt of IVS4-containing pre-mRNA and 107 nt of spliced mRNA. **(b-d)** mRNA/pre-mRNA ratio, determined using RPA probes b, c and e, as a measure of the *in vivo* RNA splicing rate for IVS1, IVS2 and IVS4, respectively. **(e-h)** RPA results showing downregulation of mRNAs that contain a PTC in the VDJ exon **(e,f)** or the C $\beta$ 2.1 exon **(g,h)**. RPA and quantification were as for **Figure 1** except that human  $\beta$ -globin was cotransfected as a control for transfection and probes b and d were used to detect transcripts harboring PTCs in the VDJ (V+) and C $\beta$ 2.1 (C+) exon, respectively. Constructs A-, E- and F- lack a PTC; AV+, EV+ and FV+ contain a VDJ-exon PTC; and constructs AC+, EC+ and FC+ contain a C $\beta$ 2.1-exon PTC. Values in **b-e,g** are means of four independent transfection experiments. Error bars, s.d.

when transcripts from stably transfected mutant and wild-type constructs with and without a PTC in the VDJ exon were analyzed (data not shown).

To analyze the effect of splicing rate under circumstances in which there is no exon skipping, we made an IVS2 3' splice-site mutant that had only a single pyrimidine-to-purine substitution, at position -6. This mutation modestly reduced the splice-site score (**Fig. 2a**, construct E) and reduced IVS2 splicing by ~40% (**Fig. 2c**, A versus E). No exon skipping was detected by northern-blot analysis, which was able to resolve the 0.4-kb difference between normally spliced and C $\beta$ 2.1-skipped mRNA (data not shown). RPA showed that the IVS2 splice-site mutation substantially decreased PTC-induced downregulation (**Fig. 2e,g**, E-/EV+ versus A-/AV+ and E-/EC+ versus A-/AC+).

To further test whether strong mRNA downregulation depends on splicing rate, we also made mutations in IVS1. To weaken the 3' splice site of IVS1, we replaced two pyrimidines with purines at positions -6 and -9 (**Supplementary Fig. 2** online, construct R). This substantially reduced its splice-acceptor score and reduced the rate of IVS1 splicing markedly (about ten-fold) (**Supplementary Fig. 2**). Northern-blot analysis showed that this mutation was severe enough to cause skipping of the VDJ exon in most transcripts (data not shown). However, some normally spliced transcripts were also produced, as detected by RPA with the use of a VDJ probe (**Supplementary Fig. 2**, probe b). RPA showed that transcripts

generated from the weakened 3' splice site were no longer strongly downregulated and were in fact barely reduced in abundance (less than two-fold) when they contained a PTC (**Supplementary Fig. 2**, compare lanes A- and AV+ with lanes R- and R+). Together with the results from the IVS2 mutants, the data indicate that reduced splicing efficiency decreases the downregulation of PTC-bearing transcripts.

At least one intron must be downstream from the PTC to trigger the downregulation of TCR $\beta$  transcripts<sup>6</sup>. This led us to hypothesize that the splicing efficiency of introns downstream from the PTC is the crucial parameter that dictates the magnitude of TCR $\beta$  NMD. Our IVS1 and IVS2 splice-site mutants did not allow us to address this hypothesis because they contained mutations that affected the splicing efficiency of not only the mutated intron but also neighboring introns. For example, the IVS2 mutations lowered the efficiency of IVS1 and IVS4 splicing (**Fig. 2b,d**). Thus, we elected to make a mutation in an intron closer to the 3' end of the gene, IVS4. We introduced a mutation in its 3' splice site, thereby lowering its splice-site score from 87.8 to 82.5 (**Fig. 3a**, construct G). This mutation effectively inhibited its splicing, causing skipping of the exon downstream of the mutation (C $\beta$ 2.3) in ~70% of the transcripts (data not shown). Importantly, the mutation selectively inhibited IVS4 splicing, not IVS1 and IVS2 splicing (**Fig. 3b-d**), allowing us to determine whether weakening a splice site downstream, but not upstream, of a stop codon would eliminate strong mRNA downregulation. We found that it did:

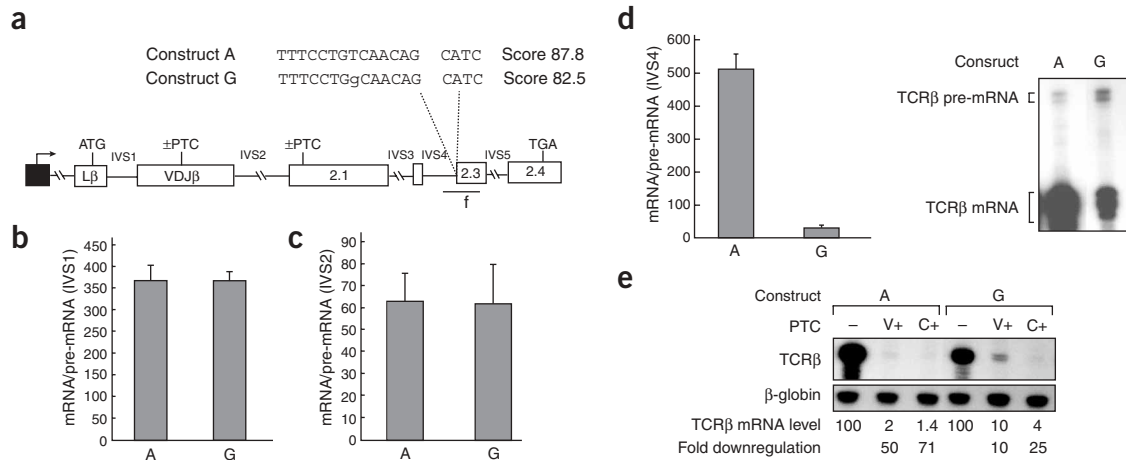


**Figure 3** A mutation in the IVS4 3' splice site reduces the downregulation of TCR $\beta$  transcripts that contain a PTC. **(a)** Schematic diagram of the wild-type (A) and mutated (G) TCR $\beta$  constructs, with their splice-site scores and intron-exon junction sequences, including the mutation (lower case). Probe f (denoted by lower-case f below the diagram) protects 133 nt of pre-mRNA and 87 nt of spliced mRNA. ATG, start codon; TGA, stop codon. **(b–d)** mRNA/pre-mRNA ratio, determined using probes b, c and f, as a measure of the *in vivo* RNA splicing rate for IVS1, IVS2 and IVS4, respectively. **d** also shows primary data from RPA using probe f. Error bars, s.d. **(e)** Results of RPA and quantification, done as for **Figure 1** except that a human  $\beta$ -globin expression plasmid was cotransfected as a control for transfection and probe b (**Fig. 2b**) was used to detect transcripts harboring PTCs in the VDJ (V+) and C $\beta$ 2.1 (C+) exons. Comparable results were obtained in two independent transfections.

the mutation reduced the downregulation of mRNAs that contained PTCs in either the VDJ or the C $\beta$ 2.1 exons (**Fig. 3e**). This provides evidence that reduced splicing efficiency downstream of a PTC is sufficient to weaken NMD.

As a further test, we examined the downregulatory response to a PTC in the penultimate (C $\beta$ 2.3) exon (**Fig. 4a**). The only intron downstream, IVS5, showed intrinsically poor splicing efficiency: the mature mRNA/IVS5+ pre-mRNA ratio was only  $\sim$ 30, compared to a mature mRNA/pre-mRNA ratio of  $\geq$ 300 for IVS1 or IVS4 (**Fig. 4b**). On the basis of this finding, we predicted that a PTC in the C $\beta$ 2.3 exon should not elicit robust downregulation. In agreement with this prediction, we found that presence of a C $\beta$ 2.3 PTC reduced TCR $\beta$  mRNA levels by only about nine-fold (**Fig. 4c**, A-/AC3+). This is much lower than the 50- to 70-fold downregulation triggered by PTCs in the upstream exons (**Fig. 3e**).

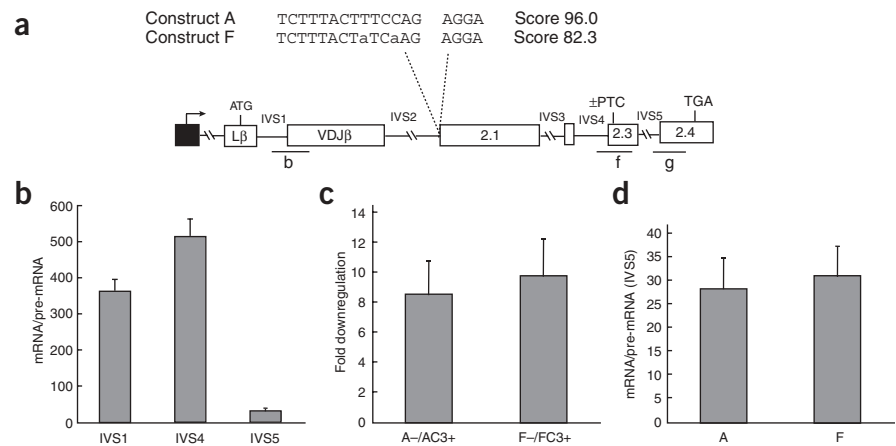
A further prediction of our hypothesis is that the splicing efficiency of introns upstream of a PTC should have no influence on NMD. To test this, we generated a construct containing an IVS2 splice-site mutation and a PTC in the penultimate exon (C $\beta$ 2.3, **Fig. 4a**). The splice-site mutation reduced the splicing efficiency of introns upstream of the C $\beta$ 2.3-exon PTC (**Fig. 2b–d**) but not downstream (**Fig. 4d**) and had no effect on mRNA downregulation elicited by the C $\beta$ 2.3-exon PTC (**Fig. 4c**, F-/FC3+). We conclude that a mutation that diminishes splicing efficiency upstream of a PTC has no effect on NMD.

### Strong downregulation conferred by efficient splicing

To elucidate whether efficient splicing is sufficient to trigger robust downregulation in response to PTCs, we determined whether we could convert a weak NMD substrate into a strong one simply by

**Figure 4** PTC position dictates whether efficient splicing promotes mRNA downregulation.

**(a)** Schematic diagram of wild-type (A) and mutated (F) TCR $\beta$  constructs, with their splice-site scores and intron-exon junction sequences, including mutations (lower case). Probes are denoted by lower-case letters below the diagram: probes b and f are as in **Figs. 2 and 3**, respectively; probe g protects 235 nt of pre-mRNA and 138 nt of spliced mRNA. ATG, start codon; TGA, stop codon. **(b)** mRNA/pre-mRNA ratio for construct A, determined using probes b, f and g, as a measure of the *in vivo* RNA splicing rate for IVS1, IVS4 and IVS5, respectively. **(c)** RPA results showing downregulation of mRNAs that contain a PTC in the C $\beta$ 2.3 exon. RPA and quantification were as for **Figure 1** except that human  $\beta$ -globin was cotransfected as a control for transfection and probe b was used. A- and F- lack a PTC; AC3+ and FC3+ contain a PTC in C $\beta$ 2.3 exon. The values charted are the means of four independent transfection experiments. **(d)** mRNA/pre-mRNA ratio, determined using probe g, as a measure of the *in vivo* RNA splicing rate. Error bars in **b–d**, s.d.



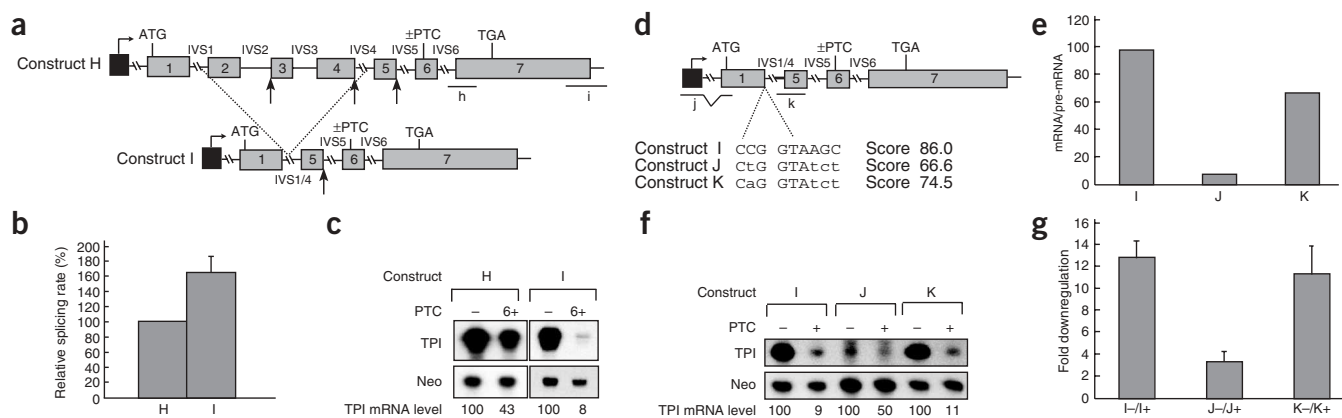


**Figure 5** Splicing efficiency dictates the magnitude of downregulation of TPI mRNAs that contain a PTC. (a) Schematic diagram of the full-length (construct H) and minigene (construct I) versions of the human TPI gene. Dashed lines indicate the region deleted from full-length TPI to generate the TPI minigene; arrows indicate the three TPI splice sites that are weaker than the weakest TCR $\beta$  splice sites. The location of the PTC in TPI exon 6 (codon 189) is shown ( $\pm$ PTC). Probes are denoted by lower-case letters below construct H: probe h protects 165 nt of pre-mRNA and 114 nt of mRNA; probe i protects 125 nt of mRNA (99 nt from the TPI 3' untranslated region and 26 nt from the vector). ATG, start codon; TGA, stop codon. (b) Relative rates of IVS6 splicing, determined in NIH 3T3 cells transfected using the calcium phosphate method<sup>50</sup>, calculated from the mRNA/pre-mRNA ratio, with the splicing rate of the wild-type transcript set to 100%. The values charted are the means of three independent transfection experiments. Error bars, s.d. (c) Results of RPAs (using probe i) performed and quantified as in **Figure 1**. 6+, PTC in exon 6. Comparable results were obtained in three independent transfection experiments. (d) Schematic diagram of the wild-type (I) and mutated (J and K) TPI minigene constructs, with their splice-site scores and intron-exon junction sequences, including mutations (lower case). Probes are denoted as lower-case letters below the diagram: probe j protects 97 nt of spliced mRNA; probe k protects 255 nt of pre-mRNA and 83 nt of spliced mRNA. (e) mRNA/pre-mRNA ratio as a measure of the *in vivo* RNA splicing rate (determined using probe k). Values are means of two independent transfection experiments. (f) RPA results and quantification, done as for **Figure 1** except that NIH 3T3 cells were transfected and probe j was used. For constructs I and K, 3  $\mu$ g of the total RNA was annealed; for construct J, 10  $\mu$ g was annealed. (g) mRNA downregulation in response to a PTC in the indicated constructs transfected in HeLa cells (determined by RPA with probe j). Values are means of four independent transfection experiments. Error bars, s.d.

increasing its splicing efficiency. We chose TPI, as it is poorly down-regulated by NMD<sup>13</sup> and many of its introns have poor splice-site scores (**Table 1**). To improve TPI splicing, we removed two of TPI's three weakest splice sites (**Fig. 5a**, arrows) by deleting the region extending from the 3' half of TPI IVS1 to the 5' half of IVS4 (construct I). RT-PCR analysis showed that this TPI minigene gave rise to mature transcripts of the size predicted if it underwent normal mRNA splicing (data not shown). The deletion improved the splicing efficiency of TPI's first intron by about six-fold (data not shown) and of its last intron by about two-fold (**Fig. 5b**). PTC-containing transcripts derived from this TPI minigene were much more strongly down-regulated than were those derived from the full-length TPI gene (**Fig. 5c**, I-/I6+ versus H-/H6+).

To directly examine whether efficient splicing is responsible for the robust downregulation of TPI minigene transcripts, we made splice-site mutations in the minigene. We first weakened the 5' splice site of the chimeric intron IVS1/4 in the TPI minigene (**Fig. 5d**, construct J). The mutation we chose markedly reduced the splice-site score (66.6 compared with 86.0 for the wild type) and effectively perturbed splicing, as shown in two ways. First, we found that this mutation caused the appearance of some exon 1-skipped transcripts, as determined by northern-blot analysis and sequence analysis of RT-PCR products (data not shown). Second, RPA showed that the mature mRNA/pre-mRNA ratio was much reduced (**Fig. 5e**). To assay mRNA downregulation, we designed an RPA probe that specifically recognized the normally spliced TPI minigene mRNA (**Fig. 5d**, probe j). Using this probe, we found that the presence of a PTC only reduced transcript levels by about two-fold. This was the case in both NIH 3T3 cells (**Fig. 5f**, lane I+ versus lane J+) and HeLa cells (**Fig. 5g**, I-/I+ versus J-/J+). NIH 3T3 cells were used because they are of murine origin and thus they lack endogenous human TPI transcripts that

complicate analysis of transfected TPI gene transcripts using some of our probes.

To determine the specificity of this response, we made a single-nucleotide substitution that substantially improved the splice-site score of the mutant (**Fig. 5d**, construct K). Although this revertant had a lower score than the parental TPI minigene construct, it was sufficient to restore splicing to an almost normal level (**Fig. 5e**). Consistent with the restored splicing rate, the reverse mutation also restored mRNA downregulation to virtually the same magnitude as the parental TPI minigene. We observed this in both NIH 3T3 cells (**Fig. 5f**, lane K+ versus lane I+) and HeLa cells (**Fig. 5g**, K-/K+ versus I-/I+).

The TPI minigene described above has a chimeric intron containing the 5' half of IVS1 fused to the 3' half of IVS4 (**Fig. 5a**). We considered the possibility that this chimeric intron is responsible for the robust downregulation of transcripts from the TPI minigene. To test this, we made a deletion that retained all of IVS1 but removed two of the three weakest TPI splice sites (**Fig. 6a**, construct L). RPA revealed that transcripts from this construct showed strong downregulation when they contained a PTC ( $\sim$ 20-fold; **Fig. 6b**, lane L- versus lane L+). Weakening of the IVS1 5' splice site by a mutation that reduced its splice-site score greatly reduced this mRNA downregulation (to about four-fold; **Fig. 6b**, M+/M- versus L+/L-). A revertant with an improved splice-site score showed improved mRNA downregulation (**Fig. 6b**, N+/N- versus M+/M-). We conclude that all of the mutations that weakened TPI splicing efficiency weakened PTC-induced downregulation and that all of the mutations that improved TPI splicing efficiency strengthened PTC-induced downregulation (**Figs. 5 and 6**).

The strong downregulatory response resulting from the large deletion that created the TPI minigene may be due to the loss of a specific negative regulatory element or to a major architectural alteration, rather than to improved splicing. To address this issue,

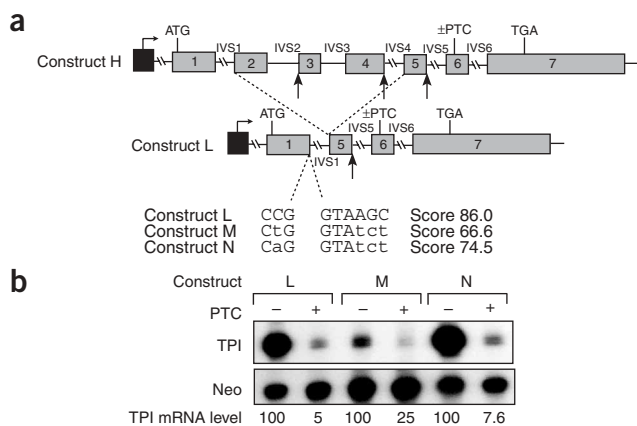


**Figure 6** The chimeric intron is not essential for strong downregulation of TPI minigene mRNAs that contain a PTC. **(a)** Schematic representations of the full-length TPI gene (construct H) and the minigene derivatives (constructs L, M and N), with their splice-site scores and intron-exon junction sequences, including mutations (lower case). The dashed lines indicate the region deleted from full-length TPI. The arrows indicate the three TPI splice sites that are weaker than the weakest TCR $\beta$  splice sites. ATG, start codon; TGA, stop codon. **(b)** RPA results and quantification done as for **Figure 1** except that probe j was used. Comparable results were obtained in two independent transfection experiments.

we made point mutations in the full-length TPI gene. We made two types of mutations predicted to improve its splicing (**Fig. 7a**, construct O). First, we mutated three of its weak splice sites to make them more similar to the consensus. Second, we mutated exon 4 to introduce additional ESEs. These mutations led to a two-fold increase in IVS4 splicing efficiency (**Fig. 7b**) and a  $\sim 30\%$  increase in IVS3 and IVS5 splicing efficiency (data not shown). Transcripts from this improved-splicing signal construct were more strongly downregulated by an exon-1 PTC (about eight-fold; lane 5 in **Fig. 7c**) than were parental TPI transcripts (about three-fold downregulation; lane 2 in **Fig. 7c**).

This improved splicing construct (construct O) gave us an opportunity to further address whether intron splicing efficiency downstream of a PTC influences NMD. To test this, we examined the effect of a PTC in exon 6 (**Fig. 7a**), which has only a single intron downstream whose splicing was not affected in construct O (**Fig. 7b**). We found that this exon-6 PTC elicited only modest mRNA downregulation of construct O (about three-fold; **Fig. 7c**, lane 6), identical to that

**Figure 7** Strengthening splicing signals elicits strong downregulation by an upstream PTC, not a downstream PTC. **(a)** Top, schematic diagram of the full-length human TPI gene. Locations of the PTCs in exon 1 (codon 23) and exon 6 (codon 189) are indicated ( $\pm$ PTC). ATG, start codon; TGA, stop codon. Arrows labeled a, b, c and d denote the positions of mutations made in construct H to generate construct O. Bottom, sequences at positions a–d, including mutations (lower case). a–c show intron-exon junction sequences and splice-site scores. d shows the sequence of nt 65–89 in exon 4 and the average frequency of ESEs in exon 4, determined using the ESE finder program (ref 15). **(b)** Relative rates of IVS4 and IVS6 splicing, determined using probe k (**Fig. 5d**) and probe h (**Fig. 5a**) with RNA from transfected NIH 3T3 cells, as in **Fig. 5b**. The values charted are the means of three independent transfection experiments. Error bars, s.d. **(c)** RPA results and quantification of the transcripts derived from the constructs shown, done as for **Figure 1** except that  $\beta$ -globin was cotransfected as a transfection control and probe j (**Fig. 5d**) was used. 1+ and 6+, PTC in exon 1 and 6, respectively. Values are the means of two independent transfection experiments.

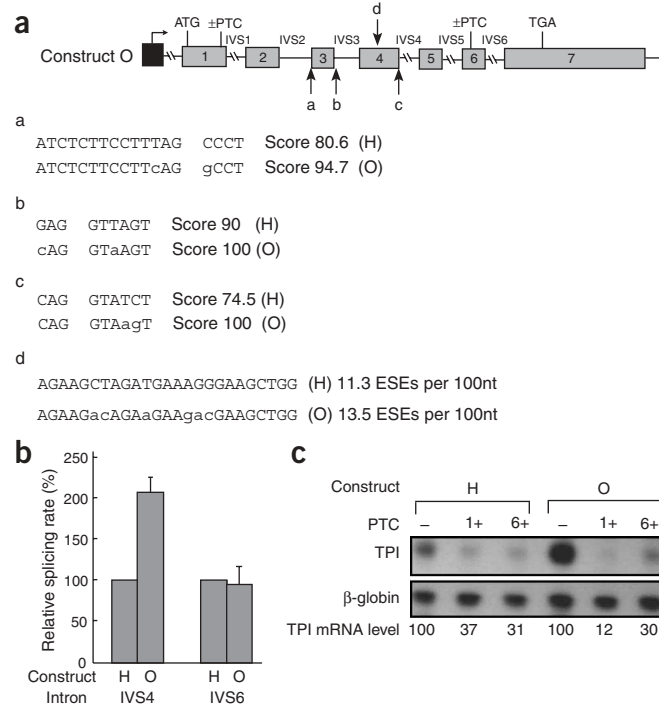
of the parental TPI gene (**Fig. 7c**, lane 3). Together with the data from the exon-1 PTC (**Fig. 7c**), this indicates that the magnitude of downregulation caused by a PTC is determined by the splicing efficiency of introns downstream of the PTC, not those upstream.

### Efficient splicing promotes translation

Because TCR $\beta$  NMD is a translation-dependent event<sup>6,14,17,18</sup> we hypothesized that efficient splicing promotes TCR $\beta$  NMD by stimulating TCR $\beta$  translation. To test this hypothesis, we compared the amount of protein produced from the parental TCR $\beta$  gene (**Fig. 1a**, construct A) with that produced from three splicing-impaired TCR $\beta$  genes described earlier (**Fig. 2a**, constructs E and F; **Fig. 3a**, construct G). We first determined protein levels by using fluorescence-activated cell sorting (FACS) analysis. Analysis of the construct bearing the weakest splicing mutation (construct E) showed that it produced markedly less protein than the parental construct (**Fig. 8a**). This difference could not be accounted for by the modest difference in mRNA levels, as protein levels were about 80–90% lower with the mutation but mRNA levels were only 20–30% lower (**Fig. 8a–c**). This was evident at all concentrations of DNA transfected. The effect of splicing efficiency on protein levels was also evident with the IVS2–splice site double mutation that strongly affected splicing (construct F) and the IVS4–splice site mutation (construct G). For some concentrations of transfected DNA, the amount of protein was so low that it was below the sensitivity limits of FACS analysis (**Fig. 8a,b**).

A summary of the effect of splicing efficiency on the translation rate predicted from protein and mRNA levels is shown in **Figure 8d**. The IVS2 mutants (constructs E and F) had greatly reduced predicted translation rates. The IVS4 mutant (construct G) had a modestly reduced predicted translation rate.

As an independent assay, we immunoprecipitated transfected cell lysates with a mouse monoclonal antibody against the V $\beta$ 8 region of TCR $\beta$ , followed by western-blot analysis with a rabbit polyclonal antibody against the C terminus of TCR $\beta$ . This assay produced essentially the same results as FACS analysis. The wild-type TCR $\beta$



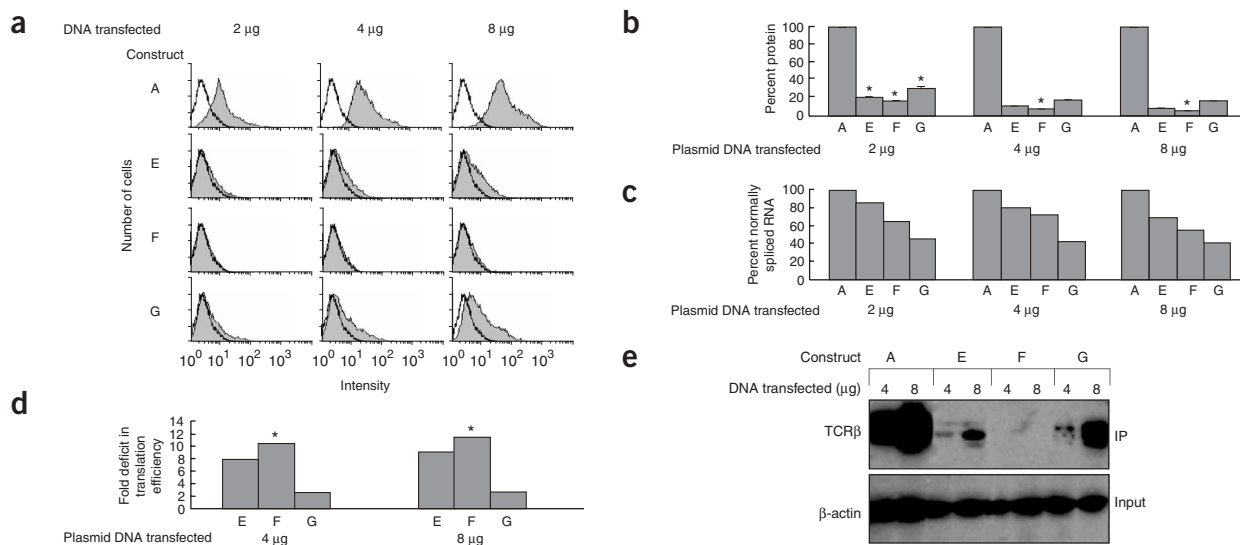


**Figure 8** Reducing splicing efficiency markedly reduces protein levels. **(a)** Expression levels of intracellular TCR $\beta$  proteins, analyzed by FACS. HeLa cells were transfected with 2, 4 or 8  $\mu$ g of wild-type TCR $\beta$  (construct A) or splicing-deficient derivatives (constructs E, F and G, shown in **Figs. 2** and **3**). Filled histograms represent the staining of TCR $\beta$  protein; open histograms represent the isotype control (background staining). **(b)** Average intracellular TCR $\beta$  protein levels (construct A level set to 100%) determined (in triplicate from a single transfection) by FACS, as in **a**. Asterisks indicate protein levels that are near background (such that protein levels might actually be lower). Comparable results were obtained in three independent transfections. Error bars, s.d. **(c)** TCR $\beta$  mRNA levels (construct A level set to 100%) measured by RPA using probe **d** (**Fig. 2a**) for constructs E and F and probe **f** (**Fig. 3a**) for construct G (these probes detect normally spliced TCR $\beta$  mRNA). Values charted are averages from two experiments. **(d)** Predicted deficit in translation efficiency of the splicing-deficient mutants as compared to the wild-type construct, calculated from the ratio of mRNA/protein levels charted in **b** and **c**. Asterisks indicate minimal values; the fold deficit in translation may be greater than that shown. **(e)** Immunoprecipitation followed by western analysis of HeLa cell lysates transfected with 4 or 8  $\mu$ g of the constructs shown.  $\beta$ -actin levels are a measure of the input. Comparable results were obtained in at least three independent transfection experiments.

construct gave a strong band of the expected size (43 kDa) after transfection of either 4 or 8  $\mu$ g plasmid DNA (**Fig. 8e**). In contrast, the three mutant constructs expressed weak or undetectable amounts of protein, even when 8  $\mu$ g of DNA was transfected (**Fig. 8e**). Comparison of the signal obtained from the splicing mutants with that from two-fold serial dilutions of the wild type showed that the amount of protein produced by each of the three mutant constructs was at least eight times lower than that produced by the wild type (data not shown). Although we cannot exclude the possibility that changes in RNA splicing efficiency alter protein levels by modifying protein stability rather than protein synthesis, this seems mechanistically improbable. Furthermore, an effect on protein stability would be inconsistent with the results reported in ref. 19, where a polysome analysis directly showed that removal of introns decreases translation efficiency. In conclusion, our results suggest that splicing efficiency has a profound effect on translation efficiency, which provides a simple explanation for the effect of splicing on the magnitude of NMD.

## DISCUSSION

TCR $\beta$  transcripts are common substrates of NMD, as most TCR $\beta$  gene rearrangements are out of frame and thus contain PTCs<sup>4,11</sup>. The truncated TCR $\beta$  proteins produced from these genes are likely to have dominant-negative effects that perturb the immune system<sup>1,4,11</sup>. Thus, we suggest that there has been strong selection pressure to efficiently downregulate TCR $\beta$  transcripts harboring PTCs. The results herein suggest that TCR $\beta$  transcripts evolved efficient RNA splicing to accomplish this goal. This notion is also supported by our finding that the TCR $\beta$  gene we used in our studies has very strong splice sites (**Table 1**), thereby allowing efficient recruitment of the spliceosomal machinery. In addition, the exons in TCR $\beta$  are rich in ESEs, the *cis*

elements that recruit serine- and arginine-rich (SR) proteins and other splicing-enhancing factors<sup>15</sup>.

Our results suggest that efficient splicing has evolved not only to increase the amount of normal protein produced but also to more effectively avoid the negative consequences of truncated proteins produced as a result of PTCs. We predict that at least three classes of genes have evolved efficient splicing to avoid the negative consequences of PTCs. One class is genes such as TCR $\beta$  that commonly acquire PTCs by mutation. This includes other immune system genes that undergo programmed rearrangement, such as TCR $\alpha$ , TCR $\gamma$ , TCR $\delta$ , I $\mu$ g, I $\mu$ l and I $\mu$ m. In support of this hypothesis, I $\mu$ m genes give rise to transcripts that are robustly downregulated (20- to 1,000-fold) when they contain PTCs<sup>20</sup>. Recently, it was shown that deletion of the 5' end of an I $\mu$ m VDJ exon prevents this robust downregulatory response<sup>21</sup>. We speculate that this region may harbor ESEs essential for efficient I $\mu$ m splicing. The second class is genes that, if prematurely terminated by mutation, encode dominant-negative proteins that unleash particularly devastating phenotypic effects. Candidate genes of this class are those transcribing mRNAs downregulated by more than the three- to five-fold range characteristic of most NMD targets, such as dihydrofolate reductase and adenine phosphoribosyl transferase<sup>22,23</sup>. The third class is genes that give rise to PTC-bearing transcripts naturally, in the absence of a mutation. Genes in this class include the surprisingly large number of genes that give rise to alternatively spliced transcripts harboring PTCs<sup>24-27</sup>. We predict that there has been selection pressure to strongly downregulate the level of these alternatively spliced PTC-bearing transcripts if they encode strong dominant-negative or deleterious gain-of-function proteins.

Our results support a model in which efficient splicing allows for more efficient translation, which in turn promotes NMD, a

translation-dependent process<sup>6,14,17,18</sup>. We believe that NMD is the target of the regulation, as enhanced splicing increased the ratio of PTC- to PTC+ transcripts under a wide variety of different contexts (Figs. 2–7). Furthermore, we found that enhanced splicing efficiency typically decreased the level of PTC+ transcripts, as expected if NMD were augmented. The decreases in PTC+ transcript levels were modest, but this was expected, as more efficient splicing generates more mature mRNA (because more pre-mRNA is spliced before it can be degraded), thereby increasing the pool of RNAs that are substrates for NMD. Nevertheless, we cannot rule out the possibility that another event in addition to NMD contributes to the increased ratio of PTC- to PTC+ mRNA resulting from efficient splicing.

Consistent with our observation that efficient splicing promotes translation, two other groups recently showed that the presence of an intron in pre-mRNA increases the translation rate of the spliced mRNA product<sup>4,19,28</sup>. The ability of an intron to stimulate translation is mediated at least in part by the EJC, a large molecular complex that requires intron splicing before it can be recruited to an mRNA<sup>3,4,9,10,19,28</sup>. To explain our results, we propose that splicing efficiency affects deposition of the EJC downstream of the stop codon. One possibility is that efficient splicing recruits the EJC more often than inefficient splicing does, thereby eliciting NMD in a greater proportion of transcripts. Alternatively, splicing efficiency may alter the EJC's binding affinity, its stability on spliced mRNA or both. In support of this, a recent study showed that mutant pre-mRNAs deficient in splicing do not colocalize with EJC proteins at the site of transcription, whereas normal pre-mRNAs do<sup>29</sup>.

Another possibility is that efficient RNA splicing might recruit a heretofore unobserved form of the EJC or a factor not yet known to be connected with splicing. Candidate factors include nucleocytoplasmic shuttling proteins that first bind mRNAs in the nucleus and then travel with them to the cytoplasm to influence their translation. Some shuttling SR proteins have these characteristics, as they are potent stimulators of translation<sup>30</sup>. In support of their involvement, it was recently shown that overexpression of the SR protein SF2/ASF stimulates NMD<sup>31</sup>. Another candidate is the 3' splice site-binding protein U2AF, which remains bound to mRNAs after splicing and travels to the cytoplasm<sup>32</sup>. Alternatively, if translation occurs in the nucleus, as some controversial evidence suggests<sup>33–35</sup>, then the novel factor may be a resident nuclear protein.

The discovery that splicing efficiency dictates the magnitude of PTC-mediated downregulation has potential implications for the treatment of human genetic diseases caused by nonsense and frameshift mutations. In cases in which the mutation generates a dominant-negative or deleterious gain-of-function protein, gene therapy approaches designed to increase the splicing efficiency of the gene may promote more efficient downregulation of the deleterious PTC-bearing allele while increasing expression from the normal allele. By contrast, if the mutation does not abrogate the normal function of the protein and hence NMD is hazardous, depressing NMD through a gene therapy approach that decreases splicing efficiency may be advantageous.

Although the results reported herein show that splicing regulates the response to PTCs, other reports have suggested that the converse also occurs—that is, that PTCs regulate splicing. For example, PTCs increase the levels of some partially spliced mRNAs and pre-mRNAs by a frame-dependent mechanism<sup>36–40</sup>. Evidence suggests that in some cases, this accumulation of unspliced and partially spliced mRNA in response to a PTC is caused by inhibition of RNA splicing<sup>36,38,40</sup>, although this was recently questioned for Igu<sup>41</sup>. In the cases of TCR $\beta$  and Igu, PTCs increase pre-mRNA levels at or near the site of transcription<sup>39</sup>, but whether this is due to inhibited splicing or

decreased degradation of precursor mRNA is not known. PTCs also increase the levels of alternatively spliced transcripts that have skipped the offending PTC<sup>42–46</sup>. Some authors have suggested that this is caused by a PTC-induced switch in splice-site selection<sup>42,43,46</sup>, although this assertion has yet to be confirmed directly. It is also possible that the increased amount of alternatively spliced transcripts results from PTCs allowing more pre-mRNA to survive decay and thereby generate more alternatively spliced transcripts. Clearly, much work is required to understand the precise nature of the cross-regulation that occurs between the RNA splicing apparatus and the translational machinery. Here we have provided a foundation for future studies by showing that splicing efficiency strongly influences the response to translation signals.

## METHODS

**Splice-site scores.** All splice-site scores were determined using Alex's splice-site score calculator (<http://www.genet.sickkids.on.ca/~ali/splicesitescoreForm.html>).

**Plasmid construction.** To generate constructs C- ( $\beta$ -974) and C+ ( $\beta$ -975), the VDJ exon was deleted, a Kpn1 site was introduced at the deletion junction by inverse PCR (using constructs B- and B+, respectively, as templates; **Supplementary Methods** online) and a PCR-amplified TPI exon 2 was subcloned into the Kpn1 and ClaI sites. Constructs D- ( $\beta$ -955) and D+ ( $\beta$ -956) were generated in the same way except that TPI exon 4 replaced the VDJ exon. Constructs E- ( $\beta$ -939), F- ( $\beta$ -984) and G- ( $\beta$ -1016) were generated by site-directed mutagenesis using A- as a template. Constructs EV+ ( $\beta$ -940), FV+ ( $\beta$ -985) and GV+ ( $\beta$ -1017) were generated in the same way using AV+ (**Supplementary Methods**) as a template, as were constructs EC+ ( $\beta$ -941), FC+ ( $\beta$ -986) and GC+ ( $\beta$ -1018) using AC+ as a template. Constructs H- (G-266) and H6+ (G-268) were described previously<sup>12</sup>. Constructs I- (G-414) and I+ (G-415) were generated by deleting nucleotides 1,222–2,572 from H- and H6+, respectively, using inverse PCR. Constructs J- (G-429) and K- (G-431) were generated by site-specific mutagenesis using I- as a template; constructs J+ (G-430) and K+ (G-432) were generated in the same way using I+ as a template. Constructs L- (G-382) and L+ (G-383) were prepared by deleting nucleotides 1,916–2,739 from H- and H6+, respectively, by inverse PCR. Constructs M- (G-427) and N- (G-433) were generated by site-specific mutagenesis using L- as a template; constructs M+ (G-428) and N+ (G-434) were generated in the same way using L+ as a template. Constructs O- (G-613), O1+ (G-614) and O6+ (G-615) were generated by site-directed mutagenesis using H-, H1+ (G-267) (ref. 12) and H6+, respectively, as templates.

All standard PCR reactions were performed with Pfu polymerase (Stratagene) at 95 °C for 3 min, followed by 30 cycles at 94 °C for 45 s, 60 °C for 90 s and 72 °C for 45 s and a final elongation step at 72 °C for 10 min. The PCR used for generating point mutations and deletions was done as previously described<sup>12,47</sup>.

**RNA isolation and RNA analysis.** Total cellular RNA was isolated as described before<sup>12</sup> or by using the Ultraspec RNA Isolation System (Biotecx). RPA was performed as described previously<sup>17</sup>, using 10  $\mu$ g RNA, unless otherwise noted. Riboprobes b and d are probes V $\beta$  and C $\beta$ , respectively, described previously<sup>48</sup>; riboprobes a, c, e, f, g, h, i and k were transcribed from PCR products subcloned into the pGEM-T easy vector (Promega); probe j was transcribed from an RT-PCR product derived from HeLa cells transfected with construct I-. Quantification of RNA levels was determined using an Instant Imager (Packard Instrumentation Company).

**Protein analysis.** Thirty-six hours after transfection, HeLa cells were trypsinized, fixed in 0.05% (v/v) paraformaldehyde for 1 h at 4 °C, permeabilized with 0.1% (v/v) Tween in PBS for 20 min at room temperature, blocked with 2.5% (v/v) FBS for 10 min at 4 °C and incubated with primary (TCR V $\beta$ F23.1 or its isotype control T 40/25) and phycoerythrin-conjugated secondary antibodies (10 min each at 4 °C after washing with 0.1% (v/v) Tween in PBS between steps). FACS analysis was performed with a FACScalibur system using CellQuest software (BD Biosciences). The mean fluorescence intensity of healthy, identically gated cells was determined after normalizing against an

isotype control for each transfection<sup>49</sup>. For immunoprecipitation and western analysis, transfected cells were trypsinized, washed in 1× PBS, pelleted, lysed for 1 h at 4 °C in 10 mM Tris HCl, 150 mM NaCl, 10 mM EDTA and 0.5% (v/v) Triton-X and centrifuged at 16,000g to pellet cellular debris. One-eighth of the total volume was used for input, the rest was pre-cleared with protein A agarose (Roche) and immunoprecipitated overnight with the TCR Vβ (F23.1) antibody and protein A agarose. Immunoprecipitates were pelleted and washed six times with Net 2 buffer (50 mM Tris-HCl, 150 mM NaCl and 0.05% (v/v) NP-40), resuspended in protein loading dye and run out on a 12% (w/v) SDS-PAGE gel, transferred to nylon membrane (Millipore), blocked with 10% (w/v) non-fat dry milk in PBS containing 0.1% Tween, incubated with an antibody to the TCR C terminus (SC9101, Santa Cruz), washed in 1× PBS-T and incubated with anti-rabbit antiserum conjugated with horseradish peroxidase (Amersham). Input samples were assessed by western-blot analysis with anti-β actin (mouse monoclonal antibody, Sigma) and HRP-conjugated sheep anti-mouse antisera. Blots were developed after reacting with ECL substrate from Pierce.

Note: Supplementary information is available on the Nature Structural & Molecular Biology website.

#### ACKNOWLEDGMENTS

We thank Y.-J. Liu and Y.-H. Wang for technical advice on FACS analysis, A. Bhalla for technical assistance and G. Cote for useful comments. This study was supported by the US National Institutes of Health grant GM058595 and the Kleberg Fund for Innovative Research Program Allocation for IRG (M.D. Anderson Cancer Center).

#### COMPETING INTERESTS STATEMENT

The authors declare that they have no competing financial interests.

Received 28 April; accepted 19 July 2005

Published online at <http://www.nature.com/nsmb/>

- Frischmeyer, P.A. & Dietz, H.C. Nonsense-mediated mRNA decay in health and disease. *Hum. Mol. Genet.* **8**, 1893–1900 (1999).
- Jacobson, A. & Peltz, S.W. Interrelationships of the pathways of mRNA decay and translation in eukaryotic cells. *Annu. Rev. Biochem.* **65**, 693–739 (1996).
- Maquat, L.E. Nonsense-mediated mRNA decay: splicing, translation and mRNP dynamics. *Nat. Rev. Mol. Cell Biol.* **5**, 89–99 (2004).
- Wilkinson, M.F. A new function for nonsense-mediated mRNA-decay factors. *Trends Genet.* **21**, 143–148 (2005).
- Holbrook, J.A., Neu-Yilik, G., Hentze, M.W. & Kulozik, A.E. Nonsense-mediated decay approaches the clinic. *Nat. Genet.* **36**, 801–808 (2004).
- Carter, M.S., Li, S. & Wilkinson, M.F. A splicing-dependent regulatory mechanism that detects translation signals. *EMBO J.* **15**, 5965–5975 (1996).
- Brocke, K.S., Neu-Yilik, G., Gehring, N.H., Hentze, M.W. & Kulozik, A.E. The human intronless melanocortin 4-receptor gene is NMD insensitive. *Hum. Mol. Genet.* **11**, 331–335 (2002).
- Maquat, L.E. & Li, X. Mammalian heat shock p70 and histone H4 transcripts, which derive from naturally intronless genes, are immune to nonsense-mediated decay. *RNA* **7**, 445–456 (2001).
- Le Hir, H., Izaurralde, E., Maquat, L.E. & Moore, M.J. The spliceosome deposits multiple proteins 20–24 nucleotides upstream of mRNA exon-exon junctions. *EMBO J.* **19**, 6860–6869 (2000).
- Wagner, E. & Lykke-Andersen, J. mRNA surveillance: the perfect persist. *J. Cell Sci.* **115**, 3033–3038 (2002).
- Li, S. & Wilkinson, M.F. Nonsense surveillance in lymphocytes? *Immunity* **8**, 135–141 (1998).
- Gudikote, J.P. & Wilkinson, M.F. T-cell receptor sequences that elicit strong down-regulation of premature termination codon-bearing transcripts. *EMBO J.* **21**, 125–134 (2002).
- Cheng, J., Fogel-Petrovic, M. & Maquat, L.E. Translation to near the distal end of the penultimate exon is required for normal levels of spliced triosephosphate isomerase mRNA. *Mol. Cell Biol.* **10**, 5215–5225 (1990).
- Carter, M.S. *et al.* A regulatory mechanism that detects premature nonsense codons in T-cell receptor transcripts *in vivo* is reversed by protein synthesis inhibitors *in vitro*. *J. Biol. Chem.* **270**, 28995–29003 (1995).
- Liu, H.X., Zhang, M. & Krainer, A.R. Identification of functional exonic splicing enhancer motifs recognized by individual SR proteins. *Genes Dev.* **12**, 1998–2012 (1998).
- Audibert, A., Weil, D. & Dautry, F. *In vivo* kinetics of mRNA splicing and transport in mammalian cells. *Mol. Cell Biol.* **22**, 6706–6718 (2002).
- Li, S., Leonard, D. & Wilkinson, M.F. T cell receptor (TCR) mini-gene mRNA expression regulated by nonsense codons: a nuclear-associated translation-like mechanism. *J. Exp. Med.* **185**, 985–992 (1997).
- Wang, J., Vock, V.M., Li, S., Olivas, O.R. & Wilkinson, M.F. A quality control pathway that down-regulates aberrant T-cell receptor (TCR) transcripts by a mechanism requiring UPF2 and translation. *J. Biol. Chem.* **277**, 18489–18493 (2002).
- Nott, A., Le Hir, H. & Moore, M.J. Splicing enhances translation in mammalian cells: an additional function of the exon junction complex. *Genes Dev.* **18**, 210–222 (2004).
- Buzina, A. & Shulman, M.J. Infrequent translation of a nonsense codon is sufficient to decrease mRNA level. *Mol. Biol. Cell* **10**, 515–524 (1999).
- Buhler, M., Paillusson, A. & Muhlemann, O. Efficient downregulation of immunoglobulin mu mRNA with premature translation-termination codons requires the 5'-half of the VDJ exon. *Nucleic Acids Res.* **32**, 3304–3315 (2004).
- Kessler, O. & Chasin, L.A. Effects of nonsense mutations on nuclear and cytoplasmic adenine phosphoribosyltransferase RNA. *Mol. Cell Biol.* **16**, 4426–4435 (1996).
- Urlaub, G., Mitchell, P.J., Ciudad, C.J. & Chasin, L.A. Nonsense mutations in the dihydrofolate reductase gene affect RNA processing. *Mol. Cell Biol.* **9**, 2868–2880 (1989).
- Lewis, B.P., Green, R.E. & Brenner, S.E. Evidence for the widespread coupling of alternative splicing and nonsense-mediated mRNA decay in humans. *Proc. Natl. Acad. Sci. USA* **100**, 189–192 (2003).
- Mendell, J.T., Sharifi, N.A., Meyers, J.L., Martinez-Murillo, F. & Dietz, H.C. Nonsense surveillance regulates expression of diverse classes of mammalian transcripts and mutes genomic noise. *Nat. Genet.* **36**, 1073–1078 (2004).
- Mitrovich, Q.M. & Anderson, P. Unproductively spliced ribosomal protein mRNAs are natural targets of mRNA surveillance in *C. elegans*. *Genes Dev.* **14**, 2173–2184 (2000).
- Morrison, M., Harris, K.S. & Roth, M.B. smg mutants affect the expression of alternatively spliced SR protein mRNAs in *Caenorhabditis elegans*. *Proc. Natl. Acad. Sci. USA* **94**, 9782–9785 (1997).
- Wiegand, H.L., Lu, S. & Cullen, B.R. Exon junction complexes mediate the enhancing effect of splicing on mRNA expression. *Proc. Natl. Acad. Sci. USA* **100**, 11327–11332 (2003).
- Custodio, N. *et al.* *In vivo* recruitment of exon junction complex proteins to transcription sites in mammalian cell nuclei. *RNA* **10**, 622–633 (2004).
- Sanford, J.R., Gray, N.K., Beckmann, K. & Caceres, J.F. A novel role for shuttling SR proteins in mRNA translation. *Genes Dev.* **18**, 755–768 (2004).
- Zhang, Z. & Krainer, A.R. Involvement of SR Proteins in mRNA Surveillance. *Mol. Cell Biol.* **16**, 597–607 (2004).
- Zolotukhin, A.S., Tan, W., Bear, J., Smulevitch, S. & Felber, B.K. U2AF participates in the binding of TAP (NXF1) to mRNA. *J. Biol. Chem.* **277**, 3935–3942 (2002).
- Dahlberg, J.E., Lund, E. & Goodwin, E.B. Nuclear translation: what is the evidence? *RNA* **9**, 1–8 (2003).
- Iborra, F.J., Jackson, D.A. & Cook, P.R. The case for nuclear translation. *J. Cell Sci.* **117**, 5713–5720 (2004).
- Wilkinson, M.F. & Shyu, A.B. RNA surveillance by nuclear scanning? *Nat. Cell Biol.* **4**, E144–E147 (2002).
- Aoufouchi, S., Yelamos, J. & Milstein, C. Nonsense mutations inhibit RNA splicing in a cell-free system: recognition of mutant codon is independent of protein synthesis. *Cell* **85**, 415–422 (1996).
- Gersappe, A., Burger, L. & Pintel, D.J. A premature termination codon in either exon of minute virus of mice P4 promoter-generated pre-mRNA can inhibit nuclear splicing of the intervening intron in an open reading frame-dependent manner. *J. Biol. Chem.* **274**, 22452–22458 (1999).
- Lozano, F., Maertzdorf, B., Pannell, R. & Milstein, C. Low cytoplasmic mRNA levels of immunoglobulin kappa light chain genes containing nonsense codons correlate with inefficient splicing. *EMBO J.* **13**, 4617–4622 (1994).
- Muhlemann, O. *et al.* Precursor RNAs harboring nonsense codons accumulate near the site of transcription. *Mol. Cell* **8**, 33–43 (2001).
- Naeger, L.K., Schoborg, R.V., Zhao, Q., Tullis, G.E. & Pintel, D.J. Nonsense mutations inhibit splicing of MVM RNA in cis when they interrupt the reading frame of either exon of the final spliced product. *Genes Dev.* **6**, 1107–1119 (1992).
- Lytle, J.R. & Steitz, J.A. Premature termination codons do not affect the rate of splicing of neighboring introns. *RNA* **10**, 657–668 (2004).
- Dietz, H.C. & Kendzior, R.J., Jr. Maintenance of an open reading frame as an additional level of scrutiny during splice site selection. *Nat. Genet.* **8**, 183–188 (1994).
- Li, B. *et al.* Stop codons affect 5' splice site selection by surveillance of splicing. *Proc. Natl. Acad. Sci. USA* **99**, 5277–5282 (2002).
- Wang, J., Chang, Y.F., Hamilton, J.I. & Wilkinson, M.F. Nonsense-associated altered splicing: a frame-dependent response distinct from nonsense-mediated decay. *Mol. Cell* **10**, 951–957 (2002).
- Wang, J., Hamilton, J.I., Carter, M.S., Li, S. & Wilkinson, M.F. Alternatively spliced TCR mRNA induced by disruption of reading frame. *Science* **297**, 108–110 (2002).
- Gersappe, A. & Pintel, D.J. A premature termination codon interferes with the nuclear function of an exon splicing enhancer in an open reading frame-dependent manner. *Mol. Cell Biol.* **19**, 1640–1650 (1999).
- Wang, J. & Wilkinson, M.F. Site-directed mutagenesis of large (13-kb) plasmids in a single-PCR procedure. *Biotechniques* **29**, 976–978 (2000).
- Wang, J., Gudikote, J.P., Olivas, O.R. & Wilkinson, M.F. Boundary-independent polar nonsense-mediated decay. *EMBO Rep.* **3**, 274–279 (2002).
- Parks, D.R. & Herzenberg, L.A. Fluorescence-activated cell sorting: theory, experimental optimization, and applications in lymphoid cell biology. *Methods Enzymol.* **108**, 197–241 (1984).
- Chen, C.A. & Okayama, H. Calcium phosphate-mediated gene transfer: a highly efficient transfection system for stably transforming cells with plasmid DNA. *Biotechniques* **6**, 632–638 (1988).